Histone fold modifications control nucleosome unwrapping and disassembly

Marek Simon[a], Justin A. North[a], John C. Shimko[b,c], Robert A. Forties[a], Michelle B. Ferdinand[b], Mridula Manohar[b], Meng Zhang[d], Richard Fishel[a,d,e], Jennifer J. Ottesen[b,c,1], and Michael G. Poirier[a,b,c,d,e,1]

[a]Department of Physics, [b]Department of Biochemistry, [c]The Ohio State Biochemistry Program, and [d]The Ohio State Biophysics Graduate Program, The Ohio State University, Columbus, OH 43210; and [e]Department of Molecular Virology, Immunology, and Medical Genetics, The Ohio State University Medical Center, Columbus, OH 43210

Nucleosomes are stable DNA–histone protein complexes that must be unwrapped and disassembled for genome expression, replication, and repair. Histone posttranslational modifications (PTMs) are major regulatory factors of these nucleosome structural changes, but the molecular mechanisms associated with PTM function remains poorly understood. Here we demonstrate that histone PTMs within distinct structured regions of the nucleosome directly regulate the inherent dynamic properties of the nucleosome. Precise PTMs were introduced into nucleosomes by chemical ligation. Single molecule magnetic tweezers measurements determined that only PTMs near the nucleosome dyad increase the rate of histone release in unwrapped nucleosomes. In contrast, FRET and restriction enzyme analysis reveal that only PTMs throughout the DNA entry–exit region increase unwrapping and enhance transcription factor binding to nucleosomal DNA. These results demonstrate that PTMs in separate structural regions of the nucleosome control distinct dynamic events, where the dyad regulates disassembly while the DNA entry–exit region regulates unwrapping. These studies are consistent with the conclusion that histone PTMs may independently influence nucleosome dynamics and associated chromatin functions.

histone acetylation | chromatin dynamics | native chemical ligation

Eukaryotic DNA is wrapped 1.65 times around histone protein octamers (1) (Fig. 1 A–C) to form nucleosomes: highly stable DNA–protein complexes with 14 separate DNA binding domains (2) and a net free energy of approximately 40 k_BT (3). This free energy poses a significant barrier to the nucleosome unwrapping and disassembly events that must occur during DNA replication, transcription, and repair (4, 5). Inherent changes to the nucleosome through histone posttranslational modifications (PTMs) are hypothesized to impact these events in cooperation with external factors such as chromatin remodeling machinery that are known to mediate nucleosome alterations (6). However, the mechanisms that underpin the regulation of nucleosome unwrapping and disassembly are not well understood.

Histone PTMs are located throughout the DNA–histone interface in several distinct regions, and genetic studies in budding yeast illustrate that amino acids at and near these modification sites influence transcriptional regulation and DNA repair (7). Histone H3 lysines 115 and 122 are simultaneously acetylated [H3 (K115acK122ac)] in the dyad region (8) and together reduce DNA–histone binding affinity and increase nucleosome sliding (9), and the acetyllysine mimics H3(K115Q) and H3(K122Q) influence transcription and DNA repair (10, 11). Mutations near the dyad result in SWI/SNF chromatin remodeling independent (SIN) transcription (12), increase nucleosome mobility (13, 14), accessibility (15), and decrease chromatin higher-order structure (16). These studies suggest histone alterations near the dyad may destabilize the nucleosome to facilitate transcription (17).

Histone H3 lysine 56 is located in the DNA entry–exit region (8, 18) and its acetylation [H3(K56ac)] is essential for DNA replication (18), repair (19), and transcriptional activation (20). H3

(K56ac) lowers H3-H4 binding affinity to DNA (21), increases DNA unwrapping (22), and enhances transcription factor binding within the nucleosome (23). These alterations in nucleosome dynamics may function at least in part to facilitate binding of DNA processing machinery.

Histone H4 lysines 77 and 79 are simultaneously acetylated [H4(K77ac,K79ac)] in the DNA–histone interface about 35 base pairs into the nucleosome (8) (Fig. 1). The acetyllysine mimics H4 (K77Q) and H4(K79Q) alter telomeric and ribosomal DNA (rDNA) silencing (24), whereas mutations at and near H4(K79) induce loss of rDNA silencing (LRS) (24). However, these LRS mutants do not result in a SIN phenotype nor influence chromatin higher-order structure (17), indicating that DNA–histone interface alterations outside of the dyad influence transcription differently than dyad alterations (17).

Together, these results suggested to us that histone PTMs throughout the DNA–histone interface could impact nucleosome dynamics and potentially influence disassembly and unwrapping. To investigate the effect of modifications in distinct structural regions on these dynamic nucleosome processes, we prepared nucleosomes with the precise histone PTMs: H3(K56ac) in the entry–exit region, H4(K77ac,K79ac) 35 base pairs into the nucleosome, and H3(K115ac,K122ac) in the dyad region. We then explored the impact of these modifications using biochemical and biophysical assays. H3(K56ac) was constructed by sequential native chemical ligation (23), whereas H3(K115ac,K122ac) and H4(K77ac,K79ac) were constructed by expressed protein ligation (9). Magnetic tweezers mechanical measurements of nucleosome arrays containing these histone PTMs revealed that only H3 (K115ac,K122ac) enhanced histone dissociation following mechanical unwrapping. Separately, FRET measurements and restriction enzyme digestion studies determined that only H3 (K56ac) and H4(K77ac,K79ac) enhance nucleosome unwrapping and protein binding to a transcription factor site embedded in nucleosomal DNA.

These results reveal that the nucleosome dyad and its PTMs facilitate nucleosome disassembly without impacting partial DNA unwrapping from the histone octamer, whereas the nucleosome DNA entry–exit region, which extends 35 base pairs into the nucleosome, regulates partial DNA unwrapping without directly impacting nucleosome disassembly. Furthermore, our observations combine to indicate that the nucleosome structure has decoupled the DNA–histone interactions that influence DNA un-
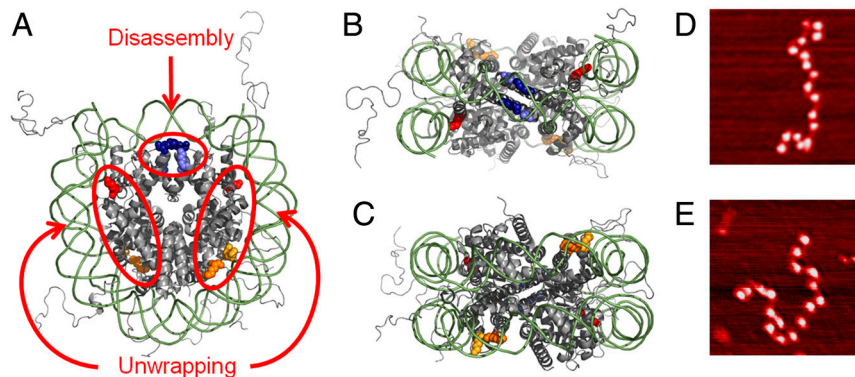
Fig. 1. *A–C* show the face, top, and bottom view of the nucleosome crystal structure (52). Acetylation sites are residues H3(K56) (red), H3(K115) (light blue), H3 (K122) (blue), H4(K77) (yellow), and H4(K79) (orange). Circles in *A* show two functionally distinct regions of the nucleosome. The dyad region of the nucleosome (top circle) regulates the final release of the histone octamer without influencing DNA unwrapping, whereas the DNA entry–exit region (bottom left and right circles) regulates the DNA unwrapping without influencing histone octamer release. (*D* and *E*) AFM images of unmodified and H3(K115ac,K122ac) nucleosome arrays, respectively. The images' width are 300 nm.

wrapping from nucleosome disassembly, which allows histone PTMs to independently influence nucleosome disassembly and unwrapping.

Results

Preparation of Nucleosome Arrays with Precise PTMs. To investigate the influence of histone PTMs on nucleosome disassembly and unwrapping, we prepared semi- and fully synthetic histones containing specific PTMs and incorporated them into single nucleosome and nucleosome arrays. H3(K115ac,K122ac) and H4 (K77ac,K79ac) were prepared by expressed protein ligation (EPL) (9), whereas H3(K56ac) was prepared by sequential native chemical ligation (NCL) (23) (Figs. S1–S3). We used ligation followed by desulfurization (25) for the syntheses of H3(K56ac) and H4(K77ac,K79ac) such that the cysteines introduced by ligation could be converted to native alanines. We reconstituted nucleosome arrays (26) with modified or unmodified purified histone octamers (27) and a 3,060 bp DNA molecule that contains 17 high-affinity nucleosome positioning sequences (NPS) and was end labeled with biotin and digoxigenin for single molecule analysis (28, 29) (Figs. S4 and S5). The arrays were purified on sucrose gradients and analyzed by atomic force microscopy (AFM) (Fig. 1 *D* and *E* and Fig. S5) and electrophoretic mobility shift assays (Fig. S6), which confirmed saturation with 17 nucleosomes (Fig. S7).

Magnetic Tweezers Measurements Quantify the Number of Nucleosomes Within a Single DNA Molecule. We used magnetic tweezers measurements to determine nucleosome retention within single nucleosome arrays while subjected to an external force (30). Nucleosomes release approximately 25 nm of DNA length when exposed to forces above 15 pN (31, 32), so we use the number of steps to measure the number of nucleosomes within the array. The arrays were extended by increasing the force to 29 pN over 100 s and then held at 29 pN for 130 s prior to relaxation. The first and fifth extensions are shown in Fig. 2*A*. Steps are observed with an average extension of 25 nm (Fig. S8) and the step number is largely preserved for five stretching cycles (Fig. 2 *A* and *E*), as previously reported (31). We confirmed full nucleosome unwrapping by observing the array extended to its contour length of 1 μm and verified the observed step number as the force is increased and held at 29 pN is representative of the nucleosome number by fitting the array's force response up to 7 pN to a polymer model (Fig. S9 and *SI Text*). We studied 31 separate unmodified nucleosome arrays with 399 nucleosomes by extending and retracting each over five cycles. The fraction of retained nucleosomes per stretch cycle fits to an exponential decay with a characteristic cycle number of 16, which converts to a 40-min dissociation time.

PTMs near the Nucleosome Dyad Facilitate Nucleosome Disassembly. To investigate the influence of histone PTMs on nucleosome stability, we extended and retracted single nucleosome arrays containing H3(K56ac) (25 arrays with 310 nucleosomes), H4 (K77ac,K79ac) (31 arrays with 372 nucleosomes), and H3 (K115ac,K122ac) (41 arrays with 476 nucleosomes) for five cycles (Fig. 2 *B–D*). We found the decay time to be 22 cycles or 55 min for H3(K56ac) nucleosome disassembly, and we observed no loss of H4(K77ac,K79ac) nucleosomes (Fig. 2*E*). In contrast, the number of observed steps in H3(K115ac,K122ac) nucleosome arrays dramatically reduced over five cycles, indicating that histone octamers dissociated at a rate of 3.4 cycles or 8.5 min (Fig. 2*E*)—a fivefold increase relative to unmodified nucleosomes. These results indicate that PTMs from the DNA entry–exit region to 35 base pairs into the nucleosome do not facilitate nucleosome disassembly following DNA unwrapping, whereas the dyad histone–DNA contacts disrupted by H3(K115ac,K122ac) are important for the maintenance of partially unwrapped nucleosomes.

PTMs Within the DNA Entry–Exit Region of the Nucleosome Facilitate DNA Unwrapping and Transcription Factor Binding. We investigated the influence of histone PTMs within the DNA–histone interface on nucleosomal DNA unwrapping and transcription factor binding using FRET (Fig. 3 and Figs. S10 and S11) and restriction enzyme digestion experiments (Figs. S12 and S13). The FRET system was designed based on previous studies (23, 33) such that the 20 base pair target sequence for a model transcription factor, LexA, is located within the nucleosome between the eighth and the 27th base pair (Fig. 3*A*). Cy3 and Cy5 fluorophores are attached to the nucleosome to monitor DNA unwrapping that is trapped as LexA is titrated in increasing concentration and binds to its target sequence (Fig. 3 *B* and *C*). To quantify DNA unwrapping, we used the unwrapping equilibrium constant, K_{eq}, which we define as the concentration ratio of partially wrapped nucleosome states that LexA can bind, to the nucleosome states that LexA cannot bind (see *SI Materials and Methods*). We determined the K_{eq} of nucleosomes containing H3(K56ac), H4(K77ac, K79ac), and H3(K115ac,K122ac) relative to unmodified nucleosomes (Fig. 3*E*). We find that H3(K56ac) and H4(K77ac,K79ac) increase K_{eq} by twofold, a biologically significant increase as in the case for dosage compensation and haploinsufficiency diseases. In contrast, H3(K115ac,K122ac) does not alter K_{eq}, which indicates that the dyad region does not impact partial DNA unwrapping.

To confirm that these results are due to DNA unwrapping rather than nucleosome sliding or repositioning, we repeated these experiments with the LexA target site on the opposite end of the

Simon et al.

Fig. 2. *A*–*D* are time series of the length of unmodified, H3(K115ac, K122ac), H3(K56ac), and H4(K77ac,K79ac) arrays, respectively, of the first (pink) and fifth extension (green). The force was increased from 7 to 29 pN and held at 29 pN (black curves). The arrows indicate step locations. (*E*) The average fraction of retained nucleosomes vs. extension–retraction cycle of unmodified (green circles), H3(K56ac) (red diamonds), H4(K77ac,K79ac) (orange triangles), and H3 (K115ac,K122ac) (blue squares) arrays. The error bars were determined from the standard deviation. Each dataset was fit to a single exponential decay: $\exp[-(\text{cycle number})/t_{\text{cycle}}]$. The t_{cycle} is 16 ± 2 cycles for unmodified arrays, 22 ± 3 cycles for H3(K56ac) arrays, and 3.4 ± 0.3 for H3(K115ac,K122ac) arrays. There was no detected change in nucleosome number with H4(K77ac,K79ac) arrays. (*F*) Diagrams of the extension–retraction cycles of unmodified, H3 (K56ac), and H3(K77ac,K79ac), and H3(K115ac,K122ac) arrays as they are extended and retracted.

DNA strand from the Cy3 fluorophore; no change in FRET was observed with increasing LexA concentration (33) (Fig. S11).

Restriction enzyme digestion experiments are an independent measure of DNA accessibility. In these studies, we reconstitute modified and unmodified histone octamers onto an NPS that places restriction enzyme target sites at specific positions along

the histone–DNA interface (34). H3(K56ac) and H4(K77ac, K79ac) increase digestion rate by threefold near the DNA entry–exit region, whereas H3(K115ac,K122ac) does not impact digestion rate by more than 1.6 times throughout the nucleosome (Figs. S12 and S13). These results are consistent with previous reports that H3(K56ac) increases DNA unwrapping (22), whereas

Fig. 3. (*A*) Nucleosome construct for measuring DNA unwrapping with and without histone PTMs. The DNA molecule is the 147 bp 601 nucleosome positioning sequence with the LexA target sequence between the eighth and 27th base pairs and is labeled with cy3 off the first base on the 5′ end. The nucleosome structure (52) shows the location of the cy3 molecule (green) and the cy5 molecules (purple). The LexA sequence is teal and histone PTMs are color coded as in Fig. 1. *B* and *C* are the fluorescent spectra of H4(K77ac,K79ac) containing nucleosomes that are excited by 510 and 610 nm, respectively, with 0 (black), 30 (blue), and 1,000 (red) mM LexA. (*D*) Normalized FRET efficiency vs. LexA concentration of unmodified (green), H3(K115ac,K122ac) (blue), H4(K77ac,K79ac) (orange), and H3(K56ac) (red) nucleosomes. The experiments were done in triplicate and the error bars are the standard deviation. The inset is an expanded scale plot of the data in *D*. (*E*) Summary of the DNA unwrapping equilibrium constant, K_{eq}, of nucleosomes with H3(K115ac,K122ac) (blue; 0.9 ± 0.2), H4(K77ac,K79ac) (orange; 1.7 ± 0.4), and H3(K56ac) (red: 1.8 ± 0.4) relative to unmodified nucleosomes.

H3(K115ac,K122ac) does not significantly influence DNA unwrapping fluctuations (9).

Discussion

In these studies, we probed the inherent properties of the nucleosome itself through perturbation of individual histone–DNA interactions throughout the nucleosome. We combined the chemical precision of EPL and NCL that allowed introduction of histone PTMs in distinct regions of the nucleosome core (35, 36) with powerful single molecule and FRET studies to provide mechanistic insight into the function of these histone PTMs within the core of the nucleosome. Our results point to two key properties of nucleosomes that impact the nucleosomal events that facilitate chromatin reorganization (Fig. 1A).

First, we find that modifications from the DNA entry–exit region to 35 base pairs into the nucleosome enhance partial DNA unwrapping without influencing disassembly. In fact, alterations in this region by histone PTMs (22), point mutations (23), and mutations in the H3 αN helix (37) enhance DNA unwrapping. These alterations appear to facilitate binding by proteins such as transcription factors without increasing nucleosome disassembly. Secondly, modifications in the nucleosome dyad region control histone octamer release following nucleosomal DNA unwrapping without directly impacting DNA unwrapping. These results suggest that alterations in the dyad region create nucleosomes that are poised for disassembly without increasing DNA accessibility. External factors that facilitate DNA unwrapping would then be required in order to initiate nucleosome disassembly.

The observation that nucleosomes have distinct regions that separately regulate nucleosome unwrapping and disassembly is consistent with the nucleosome crystal structure (2) and with a stepwise mechanism for nucleosome disassembly (38). In fact, it has previously been proposed that the numerous histone PTMs within the DNA–histone interface (8) may function to alter nucleosome stability or mobility (6, 7). Here we have defined nucleosome unwrapping as transient partial DNA unwrapping without the loss of histones, and nucleosome disassembly as the complete dissociation of the histone octamer from the DNA. By quantifying the influence of histone PTMs on DNA unwrapping and disassembly as independent events, we demonstrate that histone PTMs can significantly impact nucleosome stability and dynamics. However, these distinct processes are functionally related because DNA unwrapping is likely to occur before histone proteins disassociate from the DNA. Therefore, modifications near the entry–exit region such as H3(K56ac) or H4(K77ac,K79ac) that enhance DNA unwrapping could also indirectly facilitate nucleosome disassembly. Further studies will be required to determine if these histone PTMs function synergistically with histone PTMs in the dyad region that facilitate histone release to enhance nucleosome disassembly.

Our quantification of the impact of histone PTMs on nucleosome unwrapping and disassembly has implications for chromatin dynamics in vivo. Chromatin remodeling (39, 40) and DNA repair complexes (41, 42) unwrap and disassemble nucleosomes. Histone PTMs in the DNA–histone interface that influence these nucleosome alterations could in turn influence remodeler-induced nucleosome alterations. Recently, we reported that the mismatch repair recognition complex, hMSH2-hMSH6, disassembles nucleosomes near a mismatch (42) and that H3(K115ac,K122ac) and the acetyllysine mimic H3(K56Q) enhanced this disassembly activity by five- and twofold, respectively. Interestingly, the increase in the nucleosome disassembly rate by hMSH2-hMSH6 matches our measured fivefold change in the nucleosome disassembly rate by H3(K115ac,K122ac) and the twofold increase in DNA unwrapping by H3(K56ac). These results are consistent with a nucleosome disassembly model where multiple hMSH2-hMSH6 complexes load iteratively onto DNA at a mismatch, then freely diffuse along the duplex DNA from the mismatch (43). The finite

size of the multiple hMSH2-hMSH6 complexes would iteratively trap partially unwrapped nucleosome states until the nucleosome spontaneously disassembles (44). In this model, the enhanced DNA unwrapping by H3(K56Q) or H3(K56ac) (23) should increase the probability that hMSH2-hMSH6 traps unwrapping fluctuations and in turn increase the rate of nucleosome invasion and disassembly. In contrast, H3(K115ac,K122ac) increases the rate of histone octamer dissociation once the DNA is partially unwrapped instead of increasing the probability a nucleosome is partially unwrapped. This alteration by H3(K115ac,K122ac) should increase histone octamer release once multiple hMSH2-hMSH6 clamps have trapped a sufficient fraction of unwrapped DNA. Additional studies will be required to directly test this model of nucleosome disassembly by hMSH2-hMSH6.

ATP-dependent chromatin remodeling factors, such as SWI/SNF, are required for nucleosome disassembly for gene activation and DNA repair in vivo (39). The SWI/SNF remodeling complex appears to remodel nucleosomes by unwrapping about 50 base pairs of DNA starting from the entry–exit region (45). This remodeling is hypothesized to result in a DNA bulge that propagates along the DNA–histone interface, which repositions the nucleosome (39). Interestingly, H3(K56ac) only modestly impacts nucleosome repositioning by SWI/SNF (22), which suggests that the change in the DNA–histone interactions by H3(K56ac) is small compared to the SWI/SNF interactions with the nucleosome. In contrast, our observation that dyad PTMs facilitate histone octamer release following mechanical unwrapping suggests that combining the DNA unwrapping by SWI/SNF with the disruption of DNA–histone interactions near the dyad by PTMs will impact nucleosome remodeling. Indeed, we recently found that the introduction of negative charge and steric bulk at the nucleosome dyad by phosphorylation at H3(T118) dramatically enables nucleosome disassembly by the SWI/SNF chromatin remodeling complex (46).

Taken as a whole, our studies demonstrate that the nucleosome structure has decoupled the histone–DNA interactions that influence DNA unwrapping and histone dissociation in the nucleosome disassembly process (Fig. 1A). These studies further suggest that histone PTMs located within modular regions of the DNA–histone interface may regulate separate nucleosome structural alterations. For example, PTMs within the dyad module are poised to control nucleosome disassembly without influencing unwrapping, whereas PTMs throughout the DNA entry–exit module appear to regulate DNA unwrapping without directly influencing histone dissociation. These results suggest that unwrapping and disassembly can be tuned independently by histone modifications within the DNA–histone interface.

Materials and Methods

Histone Octamer Preparation. H3(K115ac,K122ac) and H4(K77ac,K79ac) were prepared by EPL as previously described (9). The native cysteine H3(C110) was used as the ligation site for H3(K115ac,K122ac), so the native H3 amino acid sequence was preserved. H4(A76) was used as the ligation site for H4(K77ac,K79ac), which introduced a cysteine at amino acid 76. This cysteine was converted to an alanine by desulfurization (25). H3(K56ac) was prepared by sequential native ligation as previously described (23). H3(A47) and H3(A91) were used as ligation sites, which again introduced cysteines at these amino acids. These were converted to native alanines by desulfurization (25). The semi- and fully synthetic histones were purified by HPLC and their masses were confirmed by MALDI-TOF (Figs. S1–S3). Recombinant unmodified histones H2A, H2A(K119C), H2B, H3, H3(C110A), and H4 were expressed and purified as previously described (27). Unmodified and modified histone octamers were refolded as previously described (27).

The fully synthetic histone H3(K56ac) contained the mutation C110A because of the desulfurization step. Although this mutation is often used in biochemical and biophysical studies, we recently reported that H3(C110A) slightly impacts the DNA unwrapping site accessibility within nucleosomes (23). Therefore, we always compared nucleosomes with H3(K56ac) to nucleosomes with H3(C110A), whereas nucleosomes containing H3(K115ac,K122ac) or H4(K77ac,K79ac) were compared to nucleosomes containing H3(C110).

Nucleosome Array Preparation. All nucleosome arrays were reconstituted with a 17-mer tandem repeat of a 148 bp variant of the 601 positioning sequence with 30 bp of linker DNA (29), which was cut out of the pUC19 plasmid with EcoRI and SphI. Biotin was attached to the tandem repeat by ligating the annealed pair of oligonucleotides: biotin-AGCTAGCTTTCAATAGCTCG and AATTCGAGCTATTGAAAGCTAGCT to the EcoRI overhang, whereas digoxigenin was attached to the tandem repeat by ligating the pair of annealed oligonucleotides: GGGCGGCGACCT-dig and AGGTCGCCGCCCCATG to the SphI overhang. The ligations were done simultaneously with excess concentration of annealed oligonucleotides to ensure that the tandem repeat did not ligate into multimers. The excess annealed oligonucleotides were purified away with a S-400 HR spin column (GE Healthcare). The remaining half of the plasmid was further digested with DdeI into seven pieces of various lengths ranging from 166 to 636 bp, which served as buffering DNA for nucleosome reconstitution.

Unmodified and modified nucleosomal arrays were reconstituted by salt double-dialysis (47) in 60 μL with 3 μg of plasmid DNA containing labeled 17-mer array, 15 μg of core particle DNA, 12 μg of purified histone octamer, 2 M NaCl, 1 mM benzamidine hydrochloride (BZA), 5 mM Tris (pH 8.0), and 0.5 mM EDTA. Recovered reconstituted nucleosome arrays were then purified on 5–40% sucrose gradients. Purified nucleosome arrays were characterized by electrophoretic mobility shift assay with a 2% polyacrylamide and 1% agarose gel in 90 mM Tris–borate and by AFM.

AFM Imaging of Nucleosome Arrays. Freshly cleaved mica surface was rinsed with ultrapure water and vigorously dried with nitrogen. Poly-D-lysine (50 μL, Sigma) at 10 ng/μL was deposited on the mica surface, incubated for 90 s, washed with 200 μL ultrapure water, and gently dried with nitrogen. Fifty microliters of purified nucleosome arrays at 0.5–1 nM in 0.2× TE (2 mM Tris, 0.2 mM EDTA, pH 8.0) were deposited on the poly-D-lysine-treated mica surface, incubated for 5 min, washed with 200 μL ultrapure water, and gently dried with nitrogen. The nucleosome arrays were then immediately imaged with a Dimension 3000 Scanning Probe Microscope (Veeco Instruments) using etched silicon nitride tips (PPP-NCH, Nanosensor) with a scan rate of 1 Hz and an amplitude set point of 0.9–1.2 V, which varied from tip to tip. The number of nucleosomes within each imaged array was determined manually.

Single Molecule Magnetic Tweezers Nucleosome Counting Experiments. All force-extension measurements were done with single nucleosome arrays tethered to antidigoxigenin-coated cover glass slides and streptavidin-coated magnetic beads (Dynabead M280, Invitrogen) in lab-built flow cells on a magnetic tweezers apparatus (30, 48, 49) (see SI Text for details). We determined the number of nucleosomes within a single array by detecting the number of steps in the array extension as the force is increased from 7.5 to 29 pN. The force was initially increased to 7.5 pN over 20 s, then increased from 7.5 to 29 pN over 100 s, and then held at 29 pN for 130 s. The tension was relaxed to 0.1 pN and held at this force for 4 min. This cycle was repeated four additional times. All bead heights were measured relative to a nearby bead fixed to the surface.

The step number and the step size were determined by Matlab analysis of each time series of the nucleosome array length. The steps were detected by calculating the convolution of a 31-point step function with 31 data points (1 s) centered about the time point of interest. This calculation resulted in a time series with a peak centered about each step. The number of peaks was determined and the center of each peak was located. The step size was then determined from the difference between the average of the 10 points before and after the step. The two adjacent points before and after the step were ignored when calculating step sizes.

FRET Measurements of Nucleosomal DNA Unwrapping. FRET measurements of DNA unwrapping were performed as previously described (33). The DNA molecules 601-LexA-left (Fig. 3A), and 601-LexA-right (Fig. S11A) were prepared by PCR with Cy3-labeled oligonucleotides from a plasmid containing the 601 positioning sequence with LexA binding site at bases 8–27 or 121–140, respectively (33). Oligonucleotides were labeled with a Cy3-NHS ester (GE healthcare) at a 5′ amino group then purified by RP-HPLC. The oligos used to amplify 601-LexA-L were Cy3-CTGGAGATACTGTATGAGCATACAGTACAA-TTGGTC and ACAGGATGTATATATCTGACACGTGCCTGGAGACTA; 601-LexA-R were Cy3-CTGGAGAATCCCGGTGCCGA and CTCCATACTGTATGCTCATACAG-TAATCCTGT.

H2A(K119C) was labeled before or after histone octamer refolding with Cy5-maleamide (GE Healthcare) as previously described (23). Nucleosomes were reconstituted by salt double dialysis (47) with 7 μg of DNA and 5 μg of histone octamer in 50 μL of 0.5× TE (pH 8.0), 2 M NaCl, and 1 mM BZA. Reconstituted nucleosomes were purified by 5–30% sucrose gradient. LexA protein was expressed and purified from the pJWL288 plasmid (gift from Jonathan Widom, Northwestern University, Evanston, IL) as previously described (50).

The equilibrium constants for site accessibility were determined from the reduction in FRET efficiency as LexA binds to its target site buried within the nucleosome (33) (Fig. 3A). FRET efficiency measurements were determined by the $(ratio)_A$ method as previously described (51) (see SI Text for details). LexA was titrated from 0 to 3 μM with 5 nM Cy3/Cy5-labeled nucleosomes in 0.5× TE. The FRET efficiency was determined by the $(ratio)_A$ method in triplicate for each LexA concentration. The average FRET efficiency vs. LexA concentration was fit to a noncooperative binding isotherm: $E = E_F + (E_0 - E_F)/(1 + [LexA]/S_{0.5})$, where E is the FRET efficiency, E_0 is the FRET efficiency without LexA, E_F is the FRET efficiency at high LexA concentration, and $S_{0.5\text{-nuc}}$ is the LexA concentration at which the FRET efficiency has been reduced by half [i.e., $E = (E_0 + E_F)/2$]. The relative equilibrium constant between the unmodified and modified nucleosome was determined as follows: Relative $K_{eq} = S_{0.5\text{-nuc-modified}}/S_{0.5\text{-nuc-unmodified}}$.

1. Kornberg RD (1974) Chromatin structure: A repeating unit of histones and DNA. *Science* 184:868–871.
2. Luger K, Mader AW, Richmond RK, Sargent DF, Richmond TJ (1997) Crystal structure of the nucleosome core particle at 2.8 A resolution. *Nature* 389:251–260.
3. Ranjith P, Yan J, Marko JF (2007) Nucleosome hopping and sliding kinetics determined from dynamics of single chromatin fibers in Xenopus egg extracts. *Proc Natl Acad Sci USA* 104:13649–13654.
4. Morrison AJ, Shen X (2009) Chromatin remodelling beyond transcription: the INO80 and SWR1 complexes. *Nat Rev Mol Cell Biol* 10:373–384.
5. Maier VK, Chioda MW, Becker PB (2008) ATP-dependent chromatosome remodeling. *Biol Chem* 389:345–352.
6. Cosgrove MS, Boeke JD, Wolberger C (2004) Regulated nucleosome mobility and the histone code. *Nat Struct Mol Biol* 11:1037–1043.
7. Mersfelder EL, Parthun MR (2006) The tale beyond the tail: Histone core domain modifications and the regulation of chromatin structure. *Nucleic Acids Res* 34:2653–2662.
8. Zhang L, Eugeni EE, Parthun MR, Freitas MA (2003) Identification of novel histone post-translational modifications by peptide mass fingerprinting. *Chromosoma* 112:77–86.
9. Manohar M, et al. (2009) Acetylation of histone H3 at the nucleosome dyad alters DNA–histone binding. *J Biol Chem* 284:23312–23321.
10. English CM, Adkins MW, Carson JJ, Churchill ME, Tyler JK (2006) Structural basis for the histone chaperone activity of Asf1. *Cell* 127:495–508.
11. Hyland EM, et al. (2005) Insights into the role of histone H3 and histone H4 core modifiable residues in Saccharomyces cerevisiae. *Mol Cell Biol* 25:10060–10070.
12. Kruger W, et al. (1995) Amino acid substitutions in the structured domains of histones H3 and H4 partially relieve the requirement of the yeast SWI/SNF complex for transcription. *Genes Dev* 9:2770–2779.
13. Flaus A, Rencurel C, Ferreira H, Wiechens N, Owen-Hughes T (2004) Sin mutations alter inherent nucleosome mobility. *EMBO J* 23:343–353.
14. Muthurajan UM, et al. (2004) Crystal structures of histone Sin mutant nucleosomes reveal altered protein-DNA interactions. *EMBO J* 23:260–271.
15. Kurumizaka H, Wolffe AP (1997) Sin mutations of histone H3: Influence on nucleosome core structure and function. *Mol Cell Biol* 17:6953–6969.
16. Horn PJ, Crowley KA, Carruthers LM, Hansen JC, Peterson CL (2002) The SIN domain of the histone octamer is essential for intramolecular folding of nucleosomal arrays. *Nat Struct Biol* 9:167–171.
17. Fry CJ, Norris A, Cosgrove M, Boeke JD, Peterson CL (2006) The LRS and SIN domains: Two structurally equivalent but functionally distinct nucleosomal surfaces required for transcriptional silencing. *Mol Cell Biol* 26:9045–9059.
18. Xu F, Zhang K, Grunstein M (2005) Acetylation in histone H3 globular domain regulates gene expression in yeast. *Cell* 121:375–385.
19. Chen CC, et al. (2008) Acetylated lysine 56 on histone H3 drives chromatin assembly after repair and signals for the completion of repair. *Cell* 134:231–243.
20. Williams SK, Truong D, Tyler JK (2008) Acetylation in the globular core of histone H3 on lysine-56 promotes chromatin disassembly during transcriptional activation. *Proc Natl Acad Sci USA* 105:9000–9005.
21. Andrews AJ, Chen X, Zevin A, Stargell LA, Luger K (2010) The histone chaperone Nap1 promotes nucleosome assembly by eliminating nonnucleosomal histone DNA interactions. *Mol Cell* 37:834–842.

Simon et al.

22. Neumann H, et al. (2009) A method for genetically installing site-specific acetylation in recombinant histones defines the effects of H3 K56 acetylation. *Mol Cell* 36:153–163.
23. Shimko JC, North JA, Bruns AN, Poirier MG, Ottesen JJ (2011) Preparation of fully synthetic histone H3 reveals that acetyl-lysine 56 facilitates protein binding within nucleosomes. *J Mol Biol* 408:187–204.
24. Park JH, Cosgrove MS, Youngman E, Wolberger C, Boeke JD (2002) A core nucleosome surface crucial for transcriptional silencing. *Nat Genet* 32:273–279.
25. Wan Q, Danishefsky SJ (2007) Free-radical-based, specific desulfurization of cysteine: A powerful advance in the synthesis of polypeptides and glycopolypeptides. *Angew Chem Int Ed Engl* 46:9248–9252.
26. Dorigo B, Schalch T, Bystricky K, Richmond TJ (2003) Chromatin fiber folding: Requirement for the histone H4 N-terminal tail. *J Mol Biol* 327:85–96.
27. Luger K, Rechsteiner TJ, Richmond TJ (1999) Preparation of nucleosome core particle from recombinant histones. *Methods Enzymol* 304:3–19.
28. Lowary PT, Widom J (1998) New DNA sequence rules for high affinity binding to histone octamer and sequence-directed nucleosome positioning. *J Mol Biol* 276:19–42.
29. Poirier MG, Bussiek M, Langowski J, Widom J (2008) Spontaneous access to DNA target sites in folded chromatin fibers. *J Mol Biol* 379:772–786.
30. Strick TR, Allemand JF, Bensimon D, Bensimon A, Croquette V (1996) The elasticity of a single supercoiled DNA molecule. *Science* 271:1835–1837.
31. Brower-Toland BD, et al. (2002) Mechanical disruption of individual nucleosomes reveals a reversible multistage release of DNA. *Proc Natl Acad Sci USA* 99:1960–1965.
32. Claudet C, Angelov D, Bouvet P, Dimitrov S, Bednar J (2005) Histone octamer instability under single molecule experiment conditions. *J Biol Chem* 280:19958–19965.
33. Li G, Widom J (2004) Nucleosomes facilitate their own invasion. *Nat Struct Mol Biol* 11:763–769.
34. Polach KJ, Widom J (1995) Mechanism of protein access to specific DNA sequences in chromatin: A dynamic equilibrium model for gene regulation. *J Mol Biol* 254:130–149.
35. Chatterjee C, Muir TW (2010) Chemical approaches for studying histone modifications. *J Biol Chem* 285:11045–11050.
36. Allis CD, Muir TW (2011) Spreading chromatin into chemical biology. *Chembiochem* 12:264–279.
37. Ferreira H, Somers J, Webster R, Flaus A, Owen-Hughes T (2007) Histone tails and the H3 alphaN helix regulate nucleosome mobility and stability. *Mol Cell Biol* 27:4037–4048.
38. Bohm V, et al. (2010) Nucleosome accessibility governed by the dimer/tetramer interface. *Nucleic Acids Res* 39:3093–3102.
39. Clapier CR, Cairns BR (2009) The biology of chromatin remodeling complexes. *Annu Rev Biochem* 78:273–304.
40. Gangaraju VK, Bartholomew B (2007) Mechanisms of ATP dependent chromatin remodeling. *Mutat Res* 618:3–17.
41. Dupaigne P, et al. (2008) Rad51 polymerization reveals a new chromatin remodeling mechanism. *PLoS One* 3:e3643.
42. Javaid S, et al. (2009) Nucleosome remodeling by hMSH2-hMSH6. *Mol Cell* 36:1086–1094.
43. Jeong C, et al. (2011) MutS switches between two fundamentally distinct clamps during mismatch repair. *Nat Struct Mol Biol* 18:379–385.
44. Forties RA, et al. (2011) A quantitative model of nucleosome dynamics. *Nucleic Acids Res*, in press.
45. Dechassa ML, et al. (2008) Architecture of the SWI/SNF-nucleosome complex. *Mol Cell Biol* 28:6010–6021.
46. North JA, et al. (2011) Phosphorylation of histone H3(T118) alters nucleosome dynamics and remodeling. *Nucleic Acids Res*, 10.1128/MCB.00693-08.
47. Thastrom A, Lowary PT, Widom J (2004) Measurement of histone-DNA interaction free energy in nucleosomes. *Methods* 33:33–44.
48. Skoko D, Wong B, Johnson RC, Marko JF (2004) Micromechanical analysis of the binding of DNA-bending proteins HMGB1, NHP6A, and HU reveals their ability to form highly stable DNA–protein complexes. *Biochemistry* 43:13867–13874.
49. Strick TR, Allemand JF, Bensimon D, Croquette V (1998) Behavior of supercoiled DNA. *Biophys J* 74:2016–2028.
50. Little JW, et al. (1994) Cleavage of LexA repressor. *Methods Enzymol* 244:266–284.
51. Clegg RM (1992) Fluorescence resonance energy transfer and nucleic acids. *Methods Enzymol* 211:353–388.
52. Richmond TJ, Davey CA (2003) The structure of DNA in the nucleosome core. *Nature* 423:145–150.